

# Deviant EEG resting-state large-scale brain network dynamics in euthymic bipolar disorder patients

Alena Damborská<sup>1,2\*</sup>, Camille Piguet<sup>3</sup>, Jean-Michel Aubry<sup>3,4</sup>, Alexandre G. Dayer<sup>3,4</sup>, Christoph M. Michel<sup>1,5</sup>, Cristina Berchio<sup>1,3</sup>

<sup>1</sup>Functional Brain Mapping Laboratory, Campus Biotech, Department of Basic Neurosciences, University of Geneva, Geneva, Switzerland

<sup>2</sup>Department of Psychiatry, Faculty of Medicine, Masaryk University and University Hospital Brno, Brno, Czech Republic

<sup>3</sup>Department of Psychiatry, Geneva University Hospital, Service of Psychiatric Specialties, Mood Disorders

<sup>4</sup>Department of Psychiatry, University of Geneva, Geneva, Switzerland

<sup>5</sup>Lemanic Biomedical Imaging Centre (CIBM), Lausanne and Geneva, Switzerland

## \* Correspondence:

Alena Damborská  
adambor@med.muni.cz

**Keywords: EEG microstates, Large-scale brain networks, Resting state, Dynamic brain activity, Bipolar disorder, High-density EEG.**

## Abstract

Background: Neuroimaging studies provide evidence for disrupted resting-state functional brain network activity in bipolar disorder (BD). Electroencephalographic (EEG) studies found altered temporal characteristics of functional EEG microstates during depressive episode within different affective disorders. Here we investigated whether euthymic patients with BD show deviant resting-state large-scale brain network dynamics as reflected by altered temporal characteristics of EEG microstates.

Methods: We used high-density EEG to explore between-group differences in duration, coverage and occurrence of EEG microstates in 17 euthymic adults with BD and 17 age- and gender-matched healthy controls.

Results: Microstate analysis revealed five microstates (A-E) in global clustering across all subjects. In patients compared to controls, we found increased occurrence and coverage of microstate A that did not significantly correlate with anxiety scores.

Conclusion: Our results provide neurophysiological evidence for altered large-scale brain network dynamics in BD patients and suggest the increased presence of A microstate to be an electrophysiological trait characteristic of BD.

## 1 Introduction

Bipolar disorder (BD) is a common and severe psychiatric disorder, with an important personal and societal burden (Cloutier et al., 2018; Eaton et al., 2012). The prevalence of bipolar disorder worldwide is considered to range between 1% and 3% (Merikangas et al., 2007). BD patients are frequently misdiagnosed and often identified at late stages of disease progression, which can lead to inadequate treatment (Hirschfeld, 2007) and worse functional prognosis (Vieta et al., 2018). A better

41 understanding of the underlying pathophysiology is needed to identify objective biomarkers of BD  
42 that would improve diagnostic and/or treatment stratification of patients.

43 Potential candidates for neurobiological biomarkers could arise from functional brain network  
44 abnormalities in BD patients. Evidence from brain imaging studies consistently points to  
45 abnormalities in circuits implicated in emotion regulation and reactivity. Particularly, attenuated  
46 frontal and enhanced limbic activations are reported in BD patients (Chen et al., 2011; Houenou et  
47 al., 2011; Kupferschmidt and Zakzanis, 2011). Interestingly, regions implicated in the  
48 pathophysiology of the disease, such as the inferior frontal gyrus, the medial prefrontal cortex  
49 (mPFC), the amygdala present altered activation patterns even in unaffected first-degree relatives of  
50 BD patients (Piguet et al., 2015), pointing toward brain alterations that could underlie disease  
51 vulnerability. Moreover, evidence from functional magnetic resonance imaging (fMRI) studies  
52 showed aberrant resting-state functional connectivity between frontal and meso-limbic areas in BD  
53 when compared to healthy controls (Vargas et al., 2013). A recently developed functional  
54 neuroanatomic model of BD suggests, more specifically, decreased connectivity between ventral  
55 prefrontal networks and limbic brain regions including the amygdala (Strakowski et al., 2012; Chase  
56 and Philips, 2016). The functional connectivity abnormalities in BD in brain areas associated with  
57 emotion processing were shown to vary with mood state. A resting-state functional connectivity  
58 study of emotion regulation networks demonstrated that subgenual anterior cingulate cortex  
59 (sgACC)-amygdala coupling is critically affected during mood episodes, and that functional  
60 connectivity of sgACC plays a pivotal role in mood normalization through its interactions with the  
61 ventrolateral PFC and posterior cingulate cortex (Rey et al., 2016). Nevertheless, although different  
62 fMRI metrics allowed to report deviant patterns of large-scale networks and altered resting-state  
63 functional connectivity (Rey et al., 2016; Wang et al., 2016) in BD, the precise temporal dynamics of  
64 the functional brain networks at rest remain to be determined.

65 Large-scale neural networks dynamically and rapidly re-organize themselves to enable efficient  
66 functioning (de Pasquale et al., 2018; Bressler and Menon, 2010). Fast dynamics of the resting-state  
67 large-scale neural networks can be studied on sub-second temporal scales with EEG microstate  
68 analysis (Pascual-Marqui et al., 1995; Van de Ville et al., 2010; Michel and Koenig, 2018). EEG  
69 microstates are defined as short periods (60-120 ms) of quasi-stable electric potential scalp  
70 topography (Lehmann et al., 1987; Koenig et al., 2002). Therefore, microstate analysis can cluster the  
71 scalp's topographies of the resting-state EEG activity into the set of a few microstate classes  
72 including the four canonical classes A-D (Michel and Koenig, 2018) and more recent additional ones  
73 (Custo et al., 2017; Bréchet et al., 2019). Since each microstate class topography reflects a coherent  
74 neuronal activity (Khanna et al., 2015; Michel and Koenig, 2018), the temporal characteristics, such  
75 as duration, occurrence and coverage, may be linked to the expression of spontaneous mental states  
76 and be representative of the contents of consciousness (Changeux and Michel, 2004; Lehmann et al.,  
77 1990). Numerous studies reported abnormalities in temporal properties of resting-state EEG  
78 microstates in neuropsychiatric disorders (for review see Khanna et al., 2015; Michel and Koenig,  
79 2018). Evidence from microstate studies suggests that altered resting-state brain network dynamics  
80 may represent a marker of risk to develop neuropsychiatric disorders (Tomescu et al., 2014, 2015;  
81 Andreou et al., 2014), may predict clinical variables of an illness (Gschwind et al., 2016), or help to  
82 assess the efficacy of a treatment (Atluri et al., 2018; Sverak et al., 2018). Only two studies  
83 investigated resting-state EEG in BD patients (Strik et al., 1995; Damborská et al., 2019). These  
84 studies examined patients during a depressive episode within different affective disorders. Adaptive  
85 segmentation of resting-state EEG showed abnormal microstate topographies and reduced overall  
86 average microstate duration in patients that met criteria for unipolar or bipolar mood disorders or for  
87 dysthymia (Strik et al., 1995). Using a *k*-means cluster analysis, an increased occurrence of

88 microstate A with depression as an effect related to the symptom severity was observed during a  
89 period of depression in unipolar and bipolar patients (Damborská et al., 2019).

90 Trait markers of BD based on neurobiological findings can be considered as biomarkers of illness  
91 (Piguet et al., 2016). These trait markers of BD can be studied during the periods of remission, or  
92 euthymia. No microstate study, however, has been performed on euthymic BD patients to the best of  
93 our knowledge. Thus, the main goal of the current study was to explore group differences between  
94 euthymic patients with BD and healthy controls in terms of resting-state EEG microstate dynamics.  
95 We hypothesized that BD patients during remission will show altered temporal characteristics of  
96 EEG microstates such as duration, coverage, and occurrence.

## 97 **2 Materials and Methods**

### 98 **2.1 Subjects**

99 Data were collected from 17 euthymic adult patients with BD and 17 healthy control (HC) subjects.  
100 The patients were recruited from the Mood Disorders Unit at the Geneva University Hospital. A  
101 snowball convenience sampling was used for the selection of the BD patients. Control subjects were  
102 recruited by general advertisement. All subjects were clinically evaluated using clinical structured  
103 interview (DIGS: Diagnostic for Genetic Studies, (Nurnberger et al., 1994). Bipolar disorder was  
104 confirmed in the experimental group by the usual assessment of the specialized program, an interview  
105 with a psychiatrist, and a semi-structured interview and relevant questionnaires with a psychologist.  
106 Exclusion criteria for all participants were a history of head injury, current alcohol or drug abuse.  
107 Additionally, a history of psychiatric or neurological illness and of any neurological comorbidity were  
108 exclusion criteria for controls and bipolar patients, respectively. Symptoms of mania and depression  
109 were evaluated using the Young Mania Rating Scale (YMRS) (Young et al., 1978) and the  
110 Montgomery-Åsberg Depression Rating Scale (MADRS) (Williams and Kobak, 2008), respectively.  
111 Participants were considered euthymic if they scored  $< 6$  on YMRS and  $< 12$  on MADRS at the time  
112 of the experiment, and were stable for at least 4 weeks before. All patients were medicated, receiving  
113 pharmacological therapy including antipsychotics, antidepressants and mood stabilizers, and had to be  
114 under stable medication for at least 4 weeks. The experimental group included both BD I ( $n = 10$ ) and  
115 BD II ( $n = 7$ ) types. Results of an event-related EEG study that was conducted on a sample partially  
116 overlapping with the current dataset showed that these patients present a dysfunctional gaze processing,  
117 results that were reported elsewhere (Berchio et al., 2017).

118 To check for possible demographic or clinical differences between groups, subject characteristics such  
119 as age, education or level of depression were compared between groups using independent  $t$ -tests.  
120 Anxiety is highly associated with bipolar disorder (Simon et al., 2004; 2007) and is a potential  
121 confounding variable when investigating microstate dynamics at rest. For example, decreased duration  
122 of EEG microstates at rest in patients with panic disorder has been reported (Wiedemann et al., 1998).  
123 To check for possible differences in anxiety symptoms, all subjects were assessed with the State-trait  
124 Anxiety Inventory (STAI) (Spielberger et al., 1970) and the scores were compared between patients  
125 and controls using independent  $t$ -tests.

126 This study was carried out in accordance with the recommendations of the Ethics Committee for  
127 Human Research of the Geneva University Hospital, with written informed consent from all subjects.  
128 All subjects gave written informed consent in accordance with the Declaration of Helsinki. The  
129 protocol was approved by the Ethics Committee for Human Research of the Geneva University  
130 Hospital, Switzerland.

### 131 **2.2 EEG recording and pre-processing**

132 The EEG was recorded with a high density 256-channel system (EGI System 200; Electrical Geodesic  
133 Inc., OR, USA), sampling rate of 1kHz, and Cz as acquisition reference. Subjects were sitting in a  
134 comfortable upright position and were instructed to stay as calm as possible, to keep their eyes closed  
135 and to relax for 5 minutes. They were asked to stay awake.

136 To remove muscular artifacts originating in the neck and face the data were reduced to 204 channels.  
137 Two to four minutes of EEG data were selected based on visual assessment of the artifacts and band-  
138 pass filtered between 1 and 40 Hz. Subsequently, in order to remove ballistocardiogram and oculo-  
139 motor artifacts, infomax-based Independent Component Analysis (Jung et al., 2000) was applied on all  
140 but one or two channels rejected due to abundant artifacts. Only components related to physiological  
141 noise, such as ballistocardiogram, saccadic eye movements, and eye blinking, were removed based on  
142 the waveform, topography and time course of the component. The cleaned EEG recordings were down-  
143 sampled to 125 Hz and the previously identified noisy channels were interpolated using a three-  
144 dimensional spherical spline (Perrin et al., 1989), and re-referenced to the average reference. All the  
145 preprocessing steps were done using MATLAB and the freely available Cartool Software 3.70  
146 (<https://sites.google.com/site/cartoolcommunity/home>), programmed by Denis Brunet.

### 147 **2.3 EEG data analysis**

148 To estimate the optimal set of topographies explaining the EEG signal, a standard microstate analysis  
149 was performed using *k*-means clustering (see Supplementary Fig. 1). The polarity of the maps was  
150 ignored in this procedure (Brunet et al., 2011; Murray et al., 2008; Pascual-Marqui et al., 1995). To  
151 determine the optimal number of clusters, we applied a meta-criterion that is a combination of seven  
152 independent optimization criteria (for details see Bréchet et al., 2019). In order to improve the signal-  
153 to-noise ratio, only the data at the time points of the local maximum of the Global Field Power (GFP)  
154 were clustered (Pascual-Marqui et al., 1995; Koenig et al., 2002; Britz et al., 2010; Tomescu et al.,  
155 2014). The GFP is a scalar measure of the strength of the scalp potential field and is calculated as the  
156 standard deviation of all electrodes at a given time point (Michel et al., 1993; Brunet et al., 2011;  
157 Murray et al., 2008). The cluster analysis was first computed at the individual level and then at global  
158 level across all participants (patients and controls), clustering each participant's representative maps.

159 In order to retrieve the temporal characteristics of the microstates, spatial correlation was calculated  
160 between every map identified at the global level and the individual subject's topographical map in  
161 every instant of the pre-processed EEG recording. Each continuous time point of the subject's EEG  
162 (not only the GFP peaks) was then assigned to the microstate class of the highest correlation, again  
163 ignoring polarity (Brunet et al., 2011; Bréchet et al., 2019; Michel and Koenig, 2018; Santarnecchi et  
164 al., 2017). Temporal smoothing parameters (window half size = 3, strength (Besag Factor) = 10)  
165 ensured that the noise during low GFP did not artificially interrupt the temporal segments of stable  
166 topography (Brunet et al., 2011; Pascual-Marqui et al., 1995). For each subject, three temporal  
167 parameters were then calculated for each of the previously identified microstates: (i) occurrence, (ii)  
168 coverage, and (iii) duration. Occurrence indicates how many times a microstate class recurs in one  
169 second. The coverage in percent represents the summed amount of time spent in a given microstate  
170 class as a portion of the whole analyzed period. The duration in milliseconds for a given microstate  
171 class indicates the amount of time that a given microstate class is continuously present. In order to  
172 assess the extent to which the representative microstate topographies explain the original EEG data,  
173 the global explained variance (GEV) was calculated as the sum of the explained variances of each  
174 microstate weighted by the GFP. Microstate analysis was performed using the freely available  
175 Cartool Software 3.70, (<https://sites.google.com/site/cartoolcommunity/home>), programmed by  
176 Denis Brunet. Mann-Whitney U test was used to investigate group differences for temporal  
177 parameters of each microstate. Multiple comparisons were corrected using the false discovery rate  
178 (FDR) method (Benjamini, 2010).



179 Spearman's rank correlations were calculated between the MADRS, YMRS, STAI-state, and STAI-  
180 trait scores and significant microstate parameters to check for possible relationships between  
181 symptoms and microstate dynamics. Statistical evaluation was performed by the routines included in  
182 the program package Statistica'13 (1984-2018, TIBCO, Software Inc, Version 13.4.0.14).

### 183 **3 Results**

184 There were no significant differences in age and level of education between the patient and the control  
185 groups. In both groups, very low mean scores on depression and mania symptoms were observed,  
186 which did not significantly differ between the two groups. BD patients showed higher scores on state  
187 and trait scales of the STAI. For all subject characteristics, see Table 1.

188 The meta-criterion used to determine the most dominant topographies revealed five resting-state  
189 microstate maps explaining 82.2 % of the global variance (Fig. 1). The topographies resembled those  
190 previously reported as A, B, C, and D maps (Khanna et al., 2015; Michel and Koenig, 2018; Koenig et  
191 al., 2002; Britz et al., 2010) and one of the three recently identified additional maps (Custo et al., 2017).  
192 We labeled these scalp maps A – E in accordance with the previous literature on microstates. The scalp  
193 topographies showed left posterior-right anterior orientation (map A), a right posterior-left anterior  
194 orientation (map B), an anterior-posterior orientation (map C), a fronto-central maximum (map D), and  
195 a parieto-occipital maximum (map E).

196 Since some microstate parameters showed a non-homogeneity of variances in the two groups (Levene's  
197 tests for coverage of the C microstate and duration of the A and C microstates;  $p < 0.01$ ), we decided to  
198 calculate Mann-Whitney U test to investigate group differences for temporal parameters of each  
199 microstate.

200 We found significant between-group differences for microstate parameters of the A and B microstates.  
201 Both microstates showed increased presence in patients in terms of occurrence and coverage. The two  
202 groups did not differ in any temporal parameter of microstates C, D, or E. The results of the temporal  
203 characteristics of each microstate are summarized in Table 2 and Figure 2.

204 The results of Spearman's rank correlation revealed a significant positive association between the  
205 coverage of the microstate B and the STAI-state ( $r = 0.40$ ) and STAI-trait ( $r = 0.54$ ) scores. The results  
206 of Spearman's rank correlation revealed a significant positive association between the occurrence of  
207 the microstate B and the STAI-trait ( $r = 0.47$ ) scores. The results of Spearman's rank correlation  
208 revealed no significant associations between the STAI-state or STAI-trait scores and the occurrence or  
209 coverage of the microstate A (all absolute  $r$ -values  $< 0.35$ ).

210 The results of Spearman's rank correlation revealed no significant associations between the MADRS  
211 and YMRS scores and the occurrence or coverage of the microstate A and B (all absolute  $r$ -values  $<$   
212  $0.30$ ).

### 213 **4 Discussion**

214 Our study presents the first evidence for altered resting-state EEG microstate dynamics in euthymic  
215 patients with bipolar disorder. Patients were stable and did not significantly differ in their depressive  
216 or manic symptomatology from healthy controls at the time of experiment. Despite this fact, they  
217 showed abnormally increased presence of microstates A and B, the latter correlating with anxiety level.  
218 The key discovery in the current study is the increased occurrence and coverage of microstate A in  
219 euthymic bipolar patients compared to healthy controls. In an earlier combined fMRI-EEG study the  
220 microstate A was associated with the auditory network (Britz et al., 2010). Moreover, generators of  
221 the functional EEG microstates were estimated in recent studies, where sources of the microstate A  
222 showed left-lateralized activity in the temporal lobe, insula, mPFC, and occipital gyri (Custo et al.,  
223 2017; Bréchet et al., 2019).

224 In the fMRI literature as well, resting-state functional connectivity alterations of the insula (Yin et al.,  
225 2018), the auditory network (Reinke et al., 2013), and the mPFC (Gong et al., 2019) were reported in  
226 BD patients. Verbal episodic memory deficits and language-related symptoms in BD patients were  
227 suggested to be associated with a diminished functional connectivity within the auditory/temporal  
228 gyrus and to be compensated by increased fronto-temporal functional connectivity (Reinke et al.,  
229 2013). The mPFC was also identified as a major locus of shared abnormality in BD and schizophrenia  
230 (Öngür et al., 2010), showing reduced default mode network connectivity from the mPFC to the  
231 hippocampus and fusiform gyrus, as well as increased connectivity between the mPFC and primary  
232 visual cortex in BD. Hypoconnectivity of the default mode network from the left posterior cingulate  
233 cortex to the bilateral mPFC and bilateral precuneus, and reduced salience connectivity of the left  
234 sgACC to the right inferior temporal gyrus in BD patients (Gong et al., 2019) was observed in  
235 unmedicated BD patients. In euthymic BD subjects compared to healthy controls, resting-state  
236 functional connectivity of the insula (Minuzzi et al., 2018) and amygdala (Li et al., 2018) to other  
237 brain regions was reported to be increased and decreased, respectively. In summary, the evidence from  
238 fMRI studies shows both hypoconnectivity (Gong et al., 2019; Öngür et al., 2010) and  
239 hyperconnectivity (Minuzzi et al., 2018; Reinke et al., 2013; Öngür et al., 2010) pointing to complex  
240 alterations of functional resting-state networks. Our findings of increased presence of the microstate A  
241 in euthymic BD patients might be related to the hyperconnectivity of the underlying networks that  
242 involve the temporal lobe, insula, mPFC, and occipital gyri.

243 Anxiety symptoms were previously associated with greater severity and impairment in bipolar disorder  
244 (Simon et al., 2004) and euthymic bipolar patients tend to present high residual level of anxiety (Albert  
245 et al., 2008), as it was the case here. No significant correlation was found between the increased anxiety  
246 scores and the increased occurrence or coverage of the microstate A. Our results therefore indicate that  
247 this alteration of microstate dynamics might represent a characteristic feature of BD that is not affected  
248 by anxiety.

249 The demonstrated alterations in microstate A dynamics during clinical remission might reflect (i) an  
250 impaired resting-state large-scale brain network dynamics as a trait characteristic of the disorder and/or  
251 (ii) a compensatory mechanism needed for clinical stabilization of the disorder.

252 Our study is the first to examine EEG microstate dynamics in BD patients during remission.  
253 Interestingly, in our recent study we showed positive associations of depressive symptoms with the  
254 occurrence of microstate A in a heterogenous group of patients with affective disorders (Damborská et  
255 al., 2019). The increased microstate A occurrence with depression as an effect related to the symptom  
256 severity (Damborská et al., 2019) and as a here demonstrated group difference of BD patients vs.  
257 controls, is not congruent with the previously reported reduced duration of the EEG microstates during  
258 a depressive episode (Strik et al., 1995). The experimental group in that study was not restricted to  
259 bipolar patients, however, and included also patients who met the criteria for unipolar depression or  
260 dysthymia. Moreover, authors examined the overall microstate duration and did not examine distinct  
261 microstates separately. These and other aspects, such as different clustering methods used, make it  
262 difficult to compare our findings with that early evidence of disrupted microstate dynamics in  
263 depression.

264 The microstate B was previously associated with the visual network (Britz et al., 2010; Custo et al.,  
265 2014, 2017; Bréchet et al., 2019). In our group of BD patients, we found an abnormally increased  
266 occurrence and coverage of microstate B that was associated with higher anxiety. Previous studies also  
267 suggest that anxiety may influence visual processing (Phelps et al., 2006; Laretzaki et al., 2010) and  
268 that connections between amygdala and visual cortex might underlie enhanced visual processing of  
269 emotionally salient stimuli in patients with social fobia (Goldin et al., 2009). Our finding of increased  
270 presence of microstate B positively associated with anxiety level in euthymic BD patients is consistent  
271 with these observations. To the best of our knowledge, there are no other studies that would aim to

272 examine in detail the relationship between anxiety and resting-state EEG microstate dynamics. An  
273 early microstate study reported decreased overall resting-state microstate duration in panic disorder  
274 (Wiedemann et al., 1998). This study, however, did not assess temporal characteristics of different  
275 microstates separately and it is therefore difficult to compare those findings with our observations.  
276 Further evidence is needed to determine, whether the increased presence of microstate B in our  
277 experimental group is a characteristic feature of BD or anxiety, or whether it is related to both  
278 conditions.

279 Changes in microstate A and B have been reported in several psychiatric conditions such as dementia,  
280 narcolepsy, multiple sclerosis, panic disorder, etc. (for review see Michel and Koenig, 2018). Increases  
281 in duration and occurrence of microstate A and B were observed in patients with multiple sclerosis  
282 (Gschwind, et al., 2016). Moreover, the changes in dynamic patterns of these two microstates, predicted  
283 depression scores and other clinical variables. It was suggested that multiple sclerosis affects the  
284 “sensory” (visual, auditory) rather than the higher-order (salience, central executive) functional  
285 networks (Michel and Koenig, 2018). Our findings of impaired dynamics in microstates A and B  
286 suggest a similar interpretation for the BD. Evidence from fMRI studies points to topographical  
287 dysbalances between the default mode and sensorimotor networks in BD patients with opposing  
288 patterns in depression and mania (Martino et al., 2016). Cyclothymic and depressive temperaments  
289 were associated with opposite changes in the sensorimotor network variability in the resting state signal  
290 measured by fractional standard deviation of Blood-Oxygen-Level Dependent signal (Conio et al.,  
291 2019). Our findings of altered microstates A and B dynamics is consistent with this fMRI evidence of  
292 impaired sensorimotor network in affective disorders, and moreover suggests that neural correlates of  
293 these deficits are prominent even during the euthymic state in BD patients.

294 In summary, results of the current study seem to indicate that dysfunctional activity of resting-state  
295 brain networks underlying A microstate is a detectable impairment in BD during an euthymic state.  
296 The presence of microstate A represents a measure that might be implicated in clinical practice.  
297 Importantly, this parameter, whose changes were observed during remission, could be potentially  
298 useful for early identification of bipolar disorder that could help better management of the disease. If  
299 future studies confirm the same pattern in prodromal or vulnerable subjects, it could also help detection  
300 of at-risk subjects and therefore the possibility for early intervention. The present study has, however,  
301 some limitations. Our low sample size made it impossible to examine any potential influence of  
302 medication on the microstate parameters by comparing patients receiving a specific drug with those  
303 not receiving it. Possible effects of medication on our results should be therefore taken into account.  
304 Due to the same reason, it was not possible to examine any potential influence of subtypes of bipolar  
305 disorder on microstate results.

## 306 **5 Conclusions**

307 Our study described altered EEG resting-state microstate temporal parameters in euthymic bipolar  
308 patients. These findings provide an insight into the resting-state global brain network dynamics in  
309 bipolar disorder. The increased presence of the A microstate might be considered as a candidate  
310 electrophysiological non-specific trait marker of BD. Nevertheless, studies examining possible  
311 interactions between microstate dynamics and BD symptoms are needed to better understand the  
312 dysfunction of large-scale brain network resting-state dynamics in this affective disorder.

## 313 **6 Table legends**

314 Table 1. <sup>a</sup>Edinburgh inventory (Oldfield, 1971); <sup>b</sup> Education levels: 1 = no high school, 2 = high school,  
315 3 = university studies

316 **7 Tables**

317 Table 1. Subject characteristics

| Characteristic                            | Healthy controls<br>(n = 17) | Bipolar patients<br>(n = 17) | <i>t</i> -value | p-value      |
|---|------------------------------|------------------------------|-----------------|--------------|
| Age: mean ± SD                            | 36.6 ± 14.5                  | 35.9 ± 11.9                  | -0.17           | 0.87         |
| Gender: male, <i>n</i>                    | 12                           | 12                           |                 |              |
| Handedness <sup>a</sup> : right, <i>n</i> | 14                           | 14                           |                 |              |
| Education <sup>b</sup> : mean ± SD        | 2.3 ± 0.6                    | 2.4 ± 0.5                    | 0.63            | 0.53         |
| MADRS: mean ± SD                          | 1.4 ± 1.6                    | 2.3 ± 2.9                    | 1.09            | 0.29         |
| YMRS: mean ± SD                           | 0.86 ± 1.4                   | 0.76 ± 1.4                   | -0.18           | 0.86         |
| STAI-state: mean ± SD                     | 26.7 ± 4.8                   | 36.9 ± 15.2                  | -2.13           | <b>0.04</b>  |
| STAI-trait: mean ± SD                     | 27.4 ± 5.2                   | 42.9 ± 13.3                  | -3.7            | <b>0.001</b> |

318

319

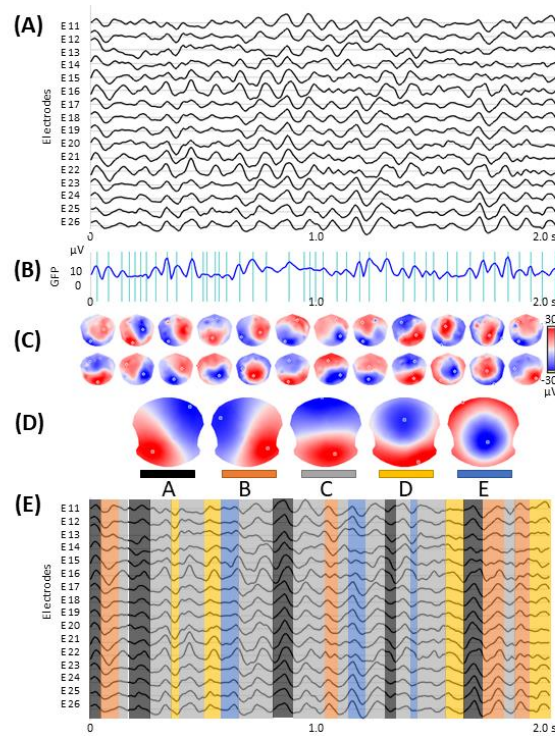
320 Table 2. Mann-Whitney U test for group comparisons in the investigated microstate parameters

| Microstate                         | A           | B           | C         | D         | E       |
|------------------------------------|-------------|-------------|-----------|-----------|---------|
| <i>Occurrence (s<sup>-1</sup>)</i> |             |             |           |           |         |
| Patients (mean±s.d.)               | 4.5±1.1     | 3.9±1.1     | 5.2±1.1   | 3.9±2.2   | 1.9±1.2 |
| Controls (mean±s.d.)               | 3.4±1.2     | 3.0±1.1     | 5.0±1.1   | 3.4±2.1   | 2.0±1.3 |
| Z-value                            | 2.51        | 2.51        | -0.03     | 0.65      | -0.14   |
| uncorrected <i>p</i> -value        | 0.01        | 0.01        | 0.97      | 0.51      | 0.89    |
| FDR corrected <i>p</i> -value      | <b>0.03</b> | <b>0.03</b> | 0.97      | 0.85      | 0.97    |
| <i>Coverage (%)</i>                |             |             |           |           |         |
| Patients (mean±s.d.)               | 18.9±6.5    | 16.0±7.8    | 25.1±8.6  | 18.5±12.3 | 6.4±5.1 |
| Controls (mean±s.d.)               | 13.3±4.9    | 11.4±6.0    | 34.7±16.8 | 17.0±12.0 | 7.0±5.3 |
| Z-value                            | 2.62        | 2.79        | -1.69     | 0.17      | -0.21   |
| uncorrected <i>p</i> -value        | 0.009       | 0.005       | 0.09      | 0.86      | 0.84    |
| FDR corrected <i>p</i> -value      | <b>0.02</b> | <b>0.02</b> | 0.15      | 0.86      | 0.86    |
| <i>Duration (ms)</i>               |             |             |           |           |         |
| Patients (mean±s.d.)               | 26±4        | 25±4        | 29±4      | 26±6      | 21±4    |
| Controls (mean±s.d.)               | 24±1        | 24±3        | 35±9      | 27±6      | 22±4    |
| Z-value                            | 1.38        | 1.03        | -2.27     | 0.17      | -0.69   |
| uncorrected <i>p</i> -value        | 0.17        | 0.30        | 0.02      | 0.86      | 0.49    |
| FDR corrected <i>p</i> -value      | 0.42        | 0.50        | 0.12      | 0.86      | 0.61    |

321



322 8 Figures

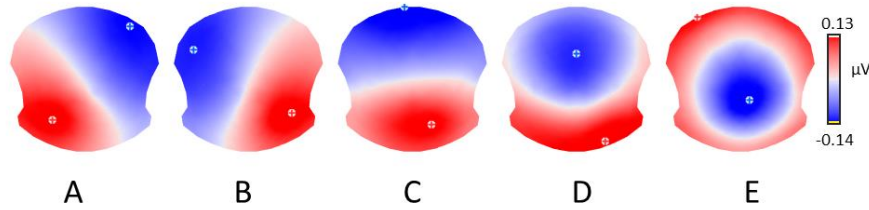


323

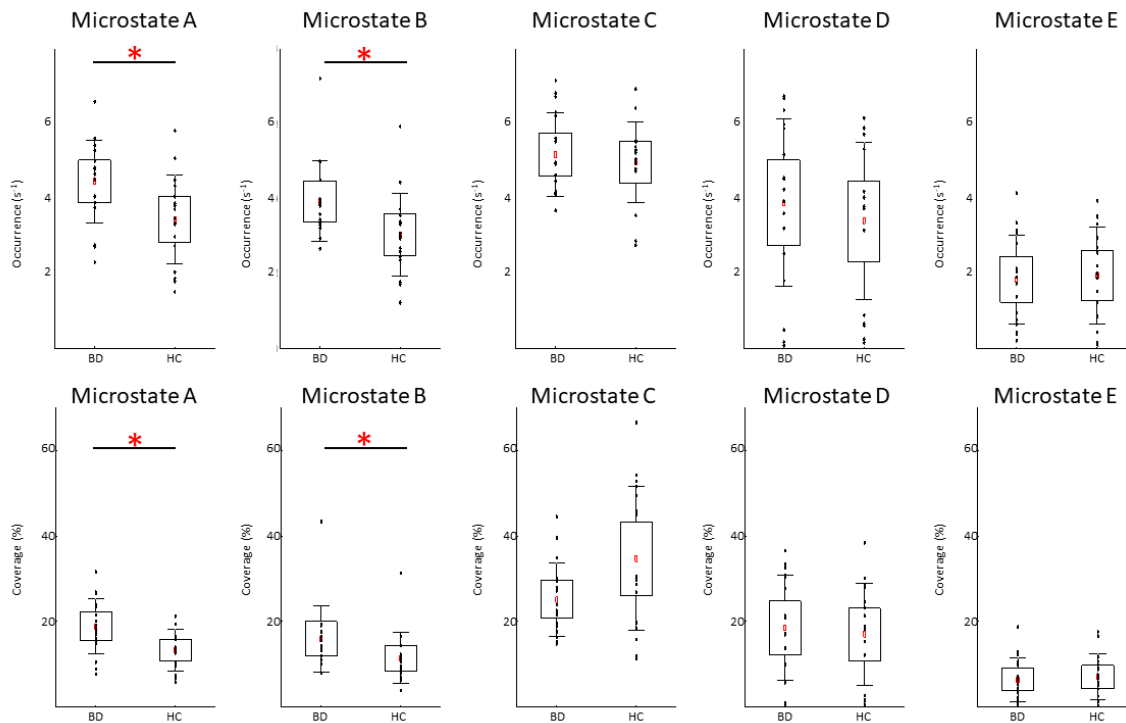
324

325 **Supplementary Figure 1.** Microstate analysis: (A) resting-state EEG from subsample of 16 out of 204  
326 electrodes; (B) global field power (GFP) curve with the GFP peaks (vertical lines) in the same EEG  
327 period as shown in (A); (C) potential maps at successive GFP peaks, indicated in (B), from the first 1  
328 s period of the recording; (D) set of five cluster maps best explaining the data as revealed by K-means  
329 clustering of the maps at the GFP peaks; (E) the original EEG recording shown in (A) with  
330 superimposed color-coded microstate segments. Note that each time point of the EEG recording was  
331 labelled with the cluster map, shown in (D), with which the instant map correlated best. The duration  
332 of segments, occurrence, and coverage for all microstates were computed on thus labeled EEG  
333 recording.

334



335  
336 Figure 1. The five microstate topographies identified in the global clustering across all subjects.  
337  
338  
339



340  
341 Figure 2. Temporal dynamics of EEG microstates in patients with bipolar disorder (BD) and in healthy  
342 controls (HC). In each subplot, the raw data is plotted on top of a boxplot showing the mean ( $\square$ ), 95%  
343 confidence interval (box plot area), 1 standard deviation (whiskers), and significant differences (\*). In  
344 all plots, x-axes represent the subject group; y-axes represent the occurrence (upper plots) or coverage  
345 (lower plots). Note significantly increased occurrence and coverage of the microstate A and B in the  
346 BD compared to HC group (FDR corrected  $p < 0.05$ ).

347 **9 Conflict of Interest**

348 The authors declare that the research was conducted in the absence of any commercial or financial  
349 relationships that could be construed as a potential conflict of interest.

350 **10 Author Contributions**

351 AD – designed the study, performed the analysis, and wrote the initial draft; JMA, AGD and CP – were  
352 responsible for clinical assessment; CMM – served as an advisor; CB – collected the HD-EEG data  
353 and was responsible for the overall oversight of the study. All authors revised the manuscript.

354 **11 Funding**

355 This project received funding from the European Union Horizon 2020 research and innovation program  
356 under the Marie Skłodowska-Curie grant agreement No. 739939. The funding source had no role in  
357 the design, collection, analysis, or interpretation of the study.

358 **12 Acknowledgments**

359 The authors wish to thank Anne Meredith Johnson for providing language help. Special thanks go to  
360 Anne-Lise Kung, psychologist, for her involvement in clinical data collection.

361 **13 References**

362 Albert, U., Rosso, G., Maina, G., Bogetto, F., (2008). Impact of anxiety disorder comorbidity on  
363 quality of life in euthymic bipolar disorder patients: differences between bipolar I and II subtypes. *J.*  
364 *Affective Disord.* 105, 297-303.

365  
366 Andreou, C., Faber, P.L., Leicht, G., Schoettle, D., Polomac, N., Hanganu-Opatz, I.L., et al. (2014).  
367 Resting-state connectivity in the prodromal phase of schizophrenia: Insights from EEG microstates.  
368 *Schizophr. Res.* 152, 513-520.

369  
370 Atluri, S., Wong, W., Moreno, S., Blumberger, D.M., Daskalakis, Z.J., Farzan, F., (2018). Selective  
371 modulation of brain network dynamics by seizure therapy in treatment-resistant depression.  
372 *NeuroImage Clin.* 20, 1176-1190.

373  
374 Benjamini Y., (2010). Discovering the false discovery rate. *J. R. Stat. Soc. Ser. B Stat. Methodol.*  
375 72, 405-416.

376  
377 Berchio C., Piguet C., Michel C.M., Cordera P., Rihs T.A., Dayer A.G., et al. (2017). Dysfunctional  
378 gaze processing in bipolar disorder. *NeuroImage Clin.* 16, 545-556.

379  
380 Bréchet, L., Brunet, D., Birot, G., Gruetter, R., Michel C.M., Jorge, J., (2019). Capturing the  
381 spatiotemporal dynamics of self-generated, task-initiated thoughts with EEG and fMRI. *Neuroimage,*  
382 194, 82-92.

383 Bressler, S.L., Menon, V., (2010) Large-scale brain networks in cognition: emerging methods and  
384 principles. *Trends Cogn. Sci.* 14, 277–290.

385

- 386 Britz, J., Van De Ville D., Michel, C.M., (2010). BOLD correlates of EEG topography reveal rapid  
387 resting-state network dynamics. *NeuroImage*, 52, 1162-1170.  
388
- 389 Brunet, D., Murray, M.M., Michel, C.M., (2011). Spatiotemporal analysis of multichannel EEG:  
390 CARTOOL. *Comput. Intell. Neurosci.* 813870  
391
- 392 Changeux, J.P. and Michel, C.M., (2004). Mechanism of neural Integration at the Brain-scale Level.  
393 In: Grillner, S., Graybiel, A.M. (Eds.), *Microcircuits*. MIT Press, Cambridge, pp. 347-370.  
394
- 395 Chase, H.W., Phillips, M.L. (2016) Elucidating Neural Network Functional Connectivity  
396 Abnormalities in Bipolar Disorder: Toward a Harmonized Methodological Approach. *Biol. Psychiatry*  
397 *Cogn. Neurosci. Neuroimaging* 1, 288-298.  
398
- 399 Chen, C.H., Suckling, J., Lennox, B.R., Ooi, C., Bullmore, E.T., (2011). A quantitative meta-analysis  
400 of fMRI studies in bipolar disorder. *Bipolar Disord.* 13, 1-15.  
401
- 402 Cloutier, M., Greene, M., Guerin, A., Touya, M., Wu, E., (2018). The economic burden of bipolar I  
403 disorder in the United States in 2015. *J. Affective Disord.*, 226, 45-51.  
404
- 405 Custo, A., Vulliemoz, S., Grouiller, F., Van De Ville, D., Michel, C., (2014). EEG source imaging of  
406 brain states using spatiotemporal regression. *Neuroimage* 96, 106-116  
407
- 408 Custo, A., Van De Ville, D., Wells, W.M., Tomescu, M.I., Brunet, D., Michel, C.M., (2017).  
409 Electroencephalographic Resting-State Networks: Source Localization of Microstates. *Brain*  
410 *Connectivity* 7, 671-682.  
411
- 412 Damborská, A., Tomescu, M.I., Honzirková, E., Barteček, R., Hořínková, J., Fedorová, S. et al. (2019)  
413 EEG resting-state large-scale brain network dynamics are related to depressive symptoms. *bioRxiv*  
414 doi: <https://doi.org/10.1101/619031>  
415
- 416 Eaton, W.W., Alexandre, P., Bienvenu, O.J., Clarke, D., Martins, S.S., Nestadt, G., et al. (2012). The  
417 Burden of Mental Disorders, in: Eaton W.W. (Ed.), *Public Mental Health*, Oxford University Press  
418
- 419 Goldin, P.R., Manber, T., Hakimi, S., Canli, T., Gross, J.J. (2009). Neural bases of social anxiety  
420 disorder: Emotional reactivity and cognitive regulation during social and physical threat. *Arch. Gen.*  
421 *Psychiatry* 66, 170-180.  
422
- 423 Gong J., Chen G., Jia Y., Zhong S., Zhao L., Luo X., et al. (2019). Disrupted functional connectivity  
424 within the default mode network and salience network in unmedicated bipolar II disorder. *Prog. Neuro-*  
425 *Psychopharmacol. Biol. Psychiatry* 88, 11-18.  
426
- 427 Gschwind, M., Hardmeier, M., Van De Ville, D., Tomescu, M.I., Penner, I., Naegelin, Y., et al. (2016).  
428 Fluctuations of spontaneous EEG topographies predict disease state in relapsing-remitting multiple  
429 sclerosis. *NeuroImage Clin.* 12, 466-477.  
430
- 431 Hirschfeld, R.M.A., (2007). Screening for bipolar disorder. *Am. J. Managed Care* 13, S164-S169.  
432



- 433 Houenou, J., Frommberger, J., Carde, S., Glasbrenner, M., Diener, C., Leboyer, M., et al. (2011).  
434 Neuroimaging-based markers of bipolar disorder: Evidence from two meta-analyses. *J. Affective*  
435 *Disord.* 132, 344-355.
- 436  
437 Jung, T., Makeig, S., Westerfield, M., Townsend, J., Courchesne, E. & Sejnowski, T. J., (2000).  
438 Removal of eye activity artifacts from visual event-related potentials in normal and clinical subjects.  
439 *Clin. Neurophysiol.* 111, 1745-1758.
- 440  
441 Khanna, A., Pascual-Leone, A., Michel, C.M., Farzan F., (2015). Microstates in resting-state EEG:  
442 Current status and future directions. *Neurosci. Biobehav. Rev.* 49, 105-113.
- 443  
444 Koenig, T., Prichep, L., Lehmann, D., Sosa, P.V., Braeker, E., Kleinlogel, H., et al. (2002). Millisecond  
445 by millisecond, year by year: Normative EEG microstates and developmental stages. *Neuroimage* 16,  
446 41-48.
- 447  
448 Kupferschmidt, D.A., Zakzanis, K.K., (2011). Toward a functional neuroanatomical signature of  
449 bipolar disorder: Quantitative evidence from the neuroimaging literature. *Psychiatry Res.*  
450 *Neuroimaging* 193, 71-79.
- 451  
452 Laretzaki, G., Plainis, S., Argyropoulos, S., Pallikaris, I.G., Bitsios, P. (2010). Threat and anxiety affect  
453 visual contrast perception. *J Psychopharmacol* 24, 667-675.
- 454  
455 Lehmann, D., Ozaki, H., Pal, I., (1987). EEG alpha map series: brain micro-states by space-oriented  
456 adaptive segmentation. *Electroencephalogr. Clin. Neurophysiol.* 67, 271-288.
- 457  
458 Lehmann D., (1990). Brain Electric Microstates and Cognition: The Atoms of Thought. In: John E.R.,  
459 Harmony T., Prichep L.S., Valdés-Sosa M., Valdés-Sosa P.A. (eds) *Machinery of the Mind.*  
460 Birkhäuser, Boston, MA, pp. 209-224.
- 461  
462 Li, G., Liu, P., Andari, E., Zhang, A., Zhang, K., (2018). The role of amygdala in patients with  
463 euthymic bipolar disorder during resting state. *Front. Psychiatry* 9(SEP).
- 464  
465 Martino, M., Magioncalda, P., Huang, Z., Conio, B., Piaggio, N., Duncan, N.W., et al. (2016).  
466 Contrasting variability patterns in the default mode and sensorimotor networks balance in bipolar  
467 depression and mania. *Proc. Natl. Acad. Sci. U S A* 113, 4824-4829.
- 468  
469 Merikangas, K.R., Akiskal, H.S., Angst, J., Greenberg, P.E., Hirschfeld, R.M.A., Petukhova, M., et al.  
470 (2007). Lifetime and 12-month prevalence of bipolar spectrum disorder in the national comorbidity  
471 survey replication. *Arch. Gen. Psychiatry* 64, 543-552.
- 472  
473 Michel, C.M., Brandeis, D., Skrandies, W., Pascual, R., Strik, W.K., Dierks, T. et al. (1993). Global  
474 field power: a 'time-honoured' index for EEG/EP map analysis. *Int. J. Psychophysiol.* 15, 1-2.
- 475  
476 Michel, C.M. and Koenig, T., (2018). EEG microstates as a tool for studying the temporal dynamics  
477 of whole-brain neuronal networks: A review. *Neuroimage* 180, 577-593.
- 478

- 479 Minuzzi, L., Syan, S.K., Smith, M., Hall, A., Hall, G.B.C., Frey, B.N., (2018). Structural and functional  
480 changes in the somatosensory cortex in euthymic females with bipolar disorder. *Aust. New Zealand J.*  
481 *Psychiatry* 52, 1075-1083.
- 482
- 483 Murray, M.M., Brunet, D., Michel, C.M., (2008). Topographic ERP analyses: A step-by-step tutorial  
484 review. *Brain Topogr.* 20, 249-264.
- 485
- 486 Nurnberger Jr., J.I., Blehar, M.C., Kaufmann, C.A., York-Cooler, C., Simpson, S.G., Harkavy-  
487 Friedman, J., et al. (1994). Diagnostic interview for genetic studies: Rationale, unique features, and  
488 training. *Arch. Gen. Psychiatry* 51, 849-859.
- 489
- 490 Oldfield, R.C., (1971). The assessment and analysis of handedness: The Edinburgh inventory.  
491 *Neuropsychologia* 9, 97-113.
- 492
- 493 Öngür, D., Lundy, M., Greenhouse, I., Shinn, A.K., Menon, V., Cohen, B.M., et al. (2010). Default  
494 mode network abnormalities in bipolar disorder and schizophrenia. *Psychiatry Res Neuroimaging*  
495 183, 59-68.
- 496
- 497 Pascual-Marqui, R.D., Michel, C.M., Lehmann, D., (1995). Segmentation of Brain Electrical Activity  
498 into Microstates; Model Estimation and Validation. *IEEE Trans. Biomed. Eng.* 42, 658-665.
- 499
- 500 de Pasquale, F., Corbetta, M., Betti, V., Della Penna, S., (2018). Cortical cores in network dynamics.  
501 *Neuroimage* 180, 370-382.
- 502
- 503 Perrin, F., Pernier, J., Bertrand, O., Echallier, J. F., (1989). Spherical splines for scalp potential and  
504 current density mapping. *Electroencephalogr. Clin. Neurophysiol.* 72, 184-187.
- 505
- 506 Phelps, E.A., Ling, S., Carrasco, M. (2006) Emotion facilitates perception and potentiates the  
507 perceptual benefits of attention. *Psychol. Sci.* 17, 292-299.
- 508
- 509 Piguet, C., Dayer, A., Aubry, J.M., (2016). Biomarkers and vulnerability to bipolar disorders.  
510 *Schweiz Arch. Neurol. Psychiatr.* 167, 57-67.
- 511
- 512 Piguet, C., Fodoulian, L., Aubry, J.M., Vuilleumier, P., Houenou, J., (2015). Bipolar disorder:  
513 Functional neuroimaging markers in relatives. *Neurosci. Biobehav. Rev.* 57, 284-296.
- 514
- 515 Reinke, B., Van de Ven, V., Matura, S., Linden, D.E.J., Oertel-Knöchel, V. (2013). Altered intrinsic  
516 functional connectivity in language-related brain regions in association with verbal memory  
517 performance in euthymic bipolar patients. *Brain Sci.* 3, 1357-1373.
- 518
- 519 Rey, G., Piguet, C., Benders, A., Favre, S., Eickhoff, S.B., Aubry, J.M., et al. (2016). Resting-state  
520 functional connectivity of emotion regulation networks in euthymic and non-euthymic bipolar  
521 disorder patients. *Eur. Psychiatry* 34, 56-63.
- 522
- 523 Santarnecchi, E., Khanna, A.R., Musaeus, C.S., Benwell, C.S.Y., Davila, P., Farzan, F., et al. (2017).  
524 EEG Microstate Correlates of Fluid Intelligence and Response to Cognitive Training. *Brain Topogr.*  
525 30, 502-520.
- 526

- 527 Simon, N.M., Otto, M.W., Wisniewski, S.R., Fossey, M., Sagduyu, K., Frank, E., et al. (2004).  
528 Anxiety disorder comorbidity in bipolar disorder patients: Data from the first 500 participants in the  
529 Systematic Treatment Enhancement Program for Bipolar Disorder (STEP-BD). *Am. J. Psychiatry*  
530 161, 2222-2229.  
531
- 532 Simon, N.M., Zalta, A.K., Otto, M.W., Ostacher, M.J., Fischmann, D., Chow, C.W., et al. (2007). The  
533 association of comorbid anxiety disorders with suicide attempts and suicidal ideation in outpatients  
534 with bipolar disorder. *J. Psychiatr. Res.* 41, 255-264.
- 535
- 536 Spielberger, C.D., Gorsuch, R.L., Lushene, R.E., (1970). *Manual for the State-Trait Anxiety*  
537 *Inventory*.  
538
- 539 Strakowski, S.M., Adler, C.M., Almeida, J., Altshuler, L.L., Blumberg, H.P., Chang, K.D., et al. (2012)  
540 The functional neuroanatomy of bipolar disorder: A consensus model. *Bipolar Disord.* 14, 313-325.
- 541
- 542 Strik, W.K., Dierks, T., Becker, T., Lehmann, D., (1995). Larger topographical variance and  
543 decreased duration of brain electric microstates in depression. *J. Neural Transmission*, 99, 213-222.  
544
- 545 Sverak, T., Albrechtova, L., Lamos, M., Rektorova, I., Ustohal, L., (2018). Intensive repetitive  
546 transcranial magnetic stimulation changes EEG microstates in schizophrenia: A pilot study.  
547 *Schizophr. Res.* 193, 451-452.
- 548
- 549 Tomescu, M.I., Rihs, T.A., Becker, R., Britz, J., Custo, A., Grouiller F., et al. (2014). Deviant dynamics  
550 of EEG resting state pattern in 22q11.2 deletion syndrome adolescents: A vulnerability marker of  
551 schizophrenia? *Schizophr. Res.* 157, 175-181.  
552
- 553 Tomescu, M.I., Rihs, T.A., Roinishvili, M., Karahanoglu, F.I., Schneider, M., Menghetti, S., et al.  
554 (2015). Schizophrenia patients and 22q11.2 deletion syndrome adolescents at risk express the same  
555 deviant patterns of resting state EEG microstates: A candidate endophenotype of schizophrenia.  
556 *Schizophr. Res. Cogn.* 2, 159-165.  
557
- 558 Van De Ville, D., Britz, J., Michel, C.M., (2010). EEG microstate sequences in healthy humans at rest  
559 reveal scale-free dynamics. *Proc. Natl. Acad. Sci.* 107, 18179–18184.  
560
- 561 Vargas, C., López-Jaramillo, C., Vieta, E., (2013). A systematic literature review of resting state  
562 network-functional MRI in bipolar disorder. *J. Affective Disord.* 150, 727-735.  
563
- 564 Vieta, E., Salagre, E., Grande, I., Carvalho, A.F., Fernandes, B.S., Berk, M., et al. (2018). Early  
565 intervention in Bipolar disorder. *Am. J. Psychiatry* 175, 411-426.  
566
- 567 Wang, Y., Zhong, S., Jia, Y., Sun, Y., Wang, B., Liu, T., et al. (2016). Disrupted resting-state  
568 functional connectivity in nonmedicated bipolar disorder. *Radiology* 280, 529-536.  
569
- 570 Wiedemann, G., Stevens, A., Pauli, P., Dengler, W., (1998). Decreased duration and altered topography  
571 of electroencephalographic microstates in patients with panic disorder. *Psychiatry Res. Neuroimaging*  
572 84, 37-48.  
573

- 574 Williams, J.B.W. and Kobak K.A., (2008). Development and reliability of a structured interview  
575 guide for the Montgomery Asberg depression rating scale (sigma). Br. J. Psychiatry 192, 52-58.  
576
- 577 Yin, Z., Chang, M., Wei, S., Jiang, X., Zhou, Y., Cui, L., et al. (2018). Decreased functional  
578 connectivity in insular subregions in depressive episodes of bipolar disorder and major depressive  
579 disorder. Front. Neurosci. 12(NOV).  
580
- 581 Young R.C., Biggs, J.T., Ziegler, V.E., Meyer, D.A., (1978). A rating scale for mania: Reliability,  
582 validity and sensitivity. Br. J. Psychiatry 133, 429-435.  
583

#### 584 **14 Data Availability Statement**

585 The raw data supporting the conclusions of this manuscript will be made available by the authors,  
586 without undue reservation, to any qualified researcher.